as Japan (8, 9). However, these virulence factors do not sufficiently clarify why only a small percentage of *H. pylori*-infected individuals develop gastric cancer.

Both *H. pylori* and some other bacteria possess γ-glutamyltranspeptidase and asparaginase, which hydrolyse glutamine and asparagine, respectively, and produce ammonia, as well as glutamate or aspartate, respectively. Both deamidases are secretory proteins that are mainly present in the periplasm and are constitutively expressed to produce glutamate and aspartate, which undergo uptake via a transporter (10). It has been previously shown that *H. pylori* γ-glutamyltranspeptidase induces apoptosis (11) and inhibits proliferation of gastric cells and T cells (11, 12). In addition, *H. pylori* asparaginase has been shown to inhibit T cell proliferation (13) and important roles in colonization by *H. pylori* of both γ-glutamyltranspeptidase and asparaginase have been demonstrated in an animal model (13–15). Although these reports have demonstrated the importance of these deamidases in the pathogenicity of *H. pylori* infection, the mechanism of γ-glutamyltranspeptidase and asparaginase in the pathogenicity of this infection remains unclear. There are several possible explanations: one is that the strong activities of γ-glutamyltranspeptidase and asparaginase cause depletion of glutamine and asparagine, which are necessary for cell proliferation, respectively (10, 16, 17). The other explanation is the production of ammonia by these deamidases, which results in damage to gastric cells (10). Glutathione is also a substrate of γ-glutamyltranspeptidase, and hydrogen peroxide produced by degradation of glutathione by γ-glutamyltranspeptidase has been suggested to cause gastric cell death (18, 19). These explanations indicate the importance of γ-glutamyltranspeptidase and asparaginase in the pathogenicity of *H. pylori*, especially in the development of gastric cancer. However, the activities of these deamidases in clinical *H. pylori* strains from patients with gastric cancer have not yet been investigated.

In this study, we analyzed clinical isolates from Japan to evaluate the relationship between the activities of γ-glutamyltranspeptidase and asparaginase in *H. pylori* and gastrointestinal diseases. In addition, we evaluated the mechanisms of these deamidase activities on inflammation of gastric cells and the effects of glutamine and asparagine on *H. pylori* infection of cells *in vitro*.

MATERIALS AND METHODS

Helicobacter pylori strains and culture conditions

Forty clinical strains were obtained from *H. pylori*-infected patients who had undergone investigative endoscopy from 2002 to 2008 at Tokyo Medical University Hospital and had diagnoses of gastric cancer ($n = 10$), gastric ulcer ($n = 10$), duodenal ulcer ($n = 10$) and chronic gastritis ($n = 10$). There were 16 women and 24 men of mean age 57.7 years (range, 24–90 years). All strains were isolated by a method described previously (20). ATCC700392 was used as a type strain of *H. pylori*, and the *ggt* gene encoding the γ-glutamyltranspeptidase knockout (Δ*ggt*) strain, the *ansB* gene encoding the asparaginase knockout (Δ*ansB*) strain, and the double-knockout (Δ*ggt*/*ansB*) strain described previously (11, 13) were used for *in vitro* infection experiments. All strains were subcultured on Brucella agar containing 5% horse blood under microaerobic conditions (5% O_2, 12% CO_2, and 83% N_2) with 95% humidity and stored in brucella broth containing 30% glycerol at −80°C until used.

γ-Glutamyltranspeptidase and asparaginase activities

γ-Glutamyltranspeptidase and asparaginase activities were determined by measuring the amount of ammonia produced by reactions with glutamine and asparagine, respectively, by phenol–hypochlorite reaction. After a 3 day incubation on blood plates, *H. pylori* cells were suspended in HEPES and the OD_{600} adjusted to 0.6. The suspension was mixed with 5 mM glutamine and 5 mM asparagine in HEPES to determine γ-glutamyltranspeptidase and asparaginase activity-ies, respectively. After a 2 hr incubation at 37°C, 20 μL suspension was mixed with 100 μL phenol nitroprusside solution (Sigma, St Louis, MO, USA) and 100 μL alkaline hypochlorite solution (Sigma). After a 30 min incubation at 37°C, the absorbance at 620 nm was measured. Each reaction was performed in duplicate. The standard curve of NH_4Cl was measured in each experiment and the activity calculated as the concentration of NH_4Cl. Statistical analyses were performed with GraphPad Prism 6 (GraphPad Software) software, using a one-way ANOVA test followed by Bonferroni's post hoc test and differences were determined to be significant when $P < 0.05$.

Expression of γ-glutamyltranspeptidase

Expression of γ-glutamyltranspeptidase was detected by western blotting using polyclonal anti-γ-glutamyltranspeptidase serum against a portion of γ-glutamyltranspeptidase from ATCC700392 as described in a previous study (21). *H. pylori* cells were grown in brucella broth containing 10% FBS to $OD_{600} = 0.5$–0.6. Cells were harvested and washed with HEPES buffer, and 50 μg protein per lane of whole cell lysate subjected to SDS–PAGE (12.5%). Proteins were transferred to PVDF membranes and the membranes blocked with PBS-T

containing 5% non-fat milk for 1 hr. After washing three times with PBS-T, the membranes were incubated with anti-γ-glutamyltranspeptidase serum (1:1000) overnight at 4°C. The membranes were then washed three times with PBS-T and incubated for 1 hr with goat anti-rabbit horseradish peroxidase-conjugated antibody (Santa Cruz Biotechnology, Santa Cruz, CA, USA; 1:5000). Signals were visualized using ECL western blotting detection reagents (GE Healthcare, Little Chalfont, UK). Band densities were measured by ImageJ 1.45s (the sum of the gray values of all the pixels in the selection divided by the number of pixels) (22). Mean band densities were compared by Sudent *t*-test using GraghPad Prism 6 and differences defined as significant when $P < 0.05$. RNA polymerase beta expression was confirmed using mouse monoclonal anti-RNA polymerase beta antibody (Abcam, Cambridge, UK).

DNA sequencing of promoter regions of γ-glutamyltranspeptidase and asparaginase

The promoter regions of the *ggt* and *ansB* genes were amplified for DNA sequencing. Based on the genome sequence of ATCC700392 (GenBank: AE000511), primers ggt F (5′-AACACGGACGCTGAAAAATC-3′) and ggt R (5′TAGCTAGCGGGTGGCTAGAA-3′), and ansB F (5′GCGCTAATGACTGCCATGAT-3′) and ansB R (5′CATGTCTTGTGAGCCGATGT-3′) were designed to amplify the promoter regions of the *ggt* and *ansB* genes, respectively. Both strands were analyzed using BigDye-Terminator version 3.1 (Applied Biosystems, Foster, CA, USA) with the same primers used for amplification.

Cell culture, *Helicobacter pylori* infection, and measurement of interleukin-8

Human gastric epithelial cell line AGS cells (ATCC CRL 1739) were obtained directly from the ATCC (Manassas, VA, USA) and maintained in Ham's F-12 medium (Sigma) containing 1 mM L-glutamine and 10% FBS at 37°C with 5% CO_2. To assay IL-8 production, AGS cells were seeded at 1×10^6 cells/mL in 24-well tissue culture dishes and *H. pylori* cells, after culturing for ~48 hr on plates, were scraped and resuspended in sterile Ham's F-12 medium to a concentration of 1×10^8 to create an multiplicity of infection of 100. AGS cells were infected by ATCC700392, the Δ*ggt* strain, the Δ*ansB* strain, or the Δ*ggt*/*ansB* strain. To determine the effects of glutamine, asparagine, and glutathione, L-glutamine (5–50 mM), asparagine (5 mM), or glutathione (10 mM) was added to the medium when the cells had been infected. After 18-hr incubation in 5% CO_2, the culture supernatants were stored until use. IL-8 in the culture supernatant was measured by ELISA using the Human CXCL8/IL-8 Quantikine ELISA Kit (R&D Systems, Minneapolis, MN, USA). Reactions were performed in duplicate. Statistical analyses were performed with GraphPad Prism 6 software, using the one-way ANOVA test followed by Bonferroni's post hoc test and differences determined to be significant when $P < 0.05$.

RESULTS

γ-Glutamyltranspeptidase and asparaginase activities in clinical *Helicobacter pylori* isolates

To compare the activities of γ-glutamyltranspeptidase and asparaginase in clinical isolates, 10 isolates each from patients with chronic gastritis, gastric ulcers, duodenal ulcers and gastric cancer were analyzed. The findings are shown in Figure 1. γ-Glutamyltranspeptidase activity of isolates from gastric cancer patients (mean value of ammonia production 1.60 mM) was significantly higher than that from those with chronic gastritis (1.23 mM, $P < 0.05$) and duodenal ulcers (1.30 mM, $P < 0.05$). Asparaginase activity was not significantly different between diseases, although the activities of the isolates from patients with gastric cancer (0.64 mM) were higher than those of isolates from patients with chronic gastritis (0.54 mM), gastric ulcers (0.54 mM) and duodenal ulcers (0.49 mM).

γ-Glutamyltranspeptidase expression in clinical *Helicobacter pylori* isolates

γ-Glutamyltranspeptidase expression was compared by western blot assay using polyclonal anti-γ-glutamyltranspeptidase serum. Seven isolates with high γ-glutamyltranspeptidase activities (range, 1.998–1.710 mM), and seven with low γ-glutamyltranspeptidase activities (range, 1.015–0.717 mM), were used for this experiment. As shown in Figure 2a, some isolates with high γ-glutamyltranspeptidase activities represented strong expression (TS1774 and TS1354) and some with low γ-glutamyltranspeptidase activities represented weak expression (S1903 and S1975). Mean band density from *H. pylori* isolates with high γ-glutamyltranspeptidase activity (mean ± SD, 57.73 ± 11.12) was significantly higher than that from *H. pylori* isolates with low γ-glutamyltranspeptidase activity (mean ± SD, 40.07 ± 7.78, $P < 0.01$), as shown in Figure 2b.

DNA sequencing of the promoter region of the *ggt* and *ansB* genes

The promoter regions of γ-glutamyltranspeptidase and asparaginase were compared between clinical isolates.

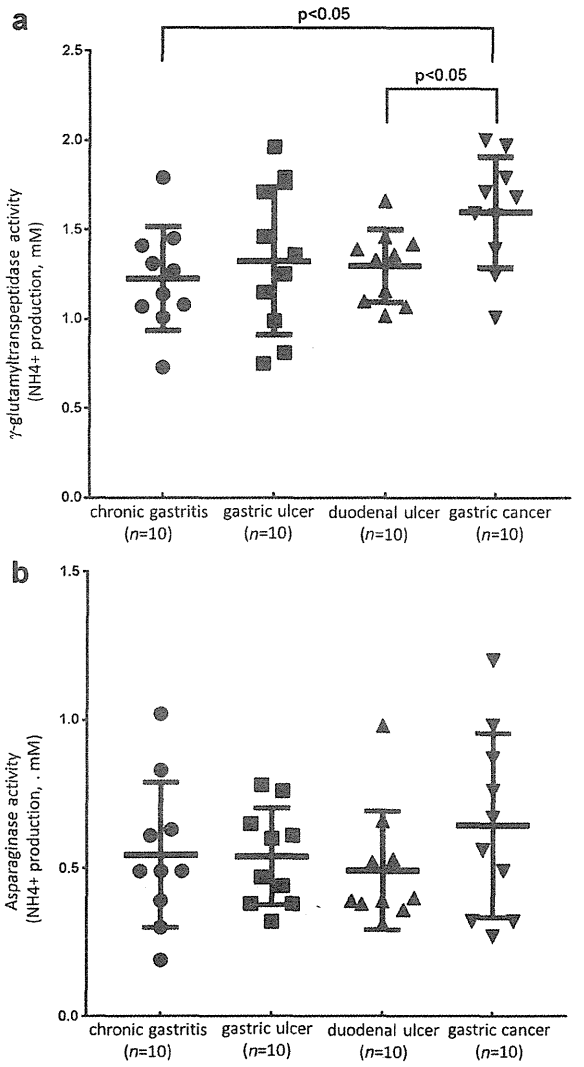

Fig. 1. Comparison of (a) γ-glutamyltranspeptidase and (b) asparaginase activities of clinical *Helicobacter pylori* isolates from patients with chronic gastritis, gastric ulcers, duodenal ulcers and gastric cancer.

Fourteen isolates (seven with strong activity and seven with weak activity), which were the same strains as were used for western blot assay for γ-glutamyltranspeptidase activity, were sequenced to compare the promoter region of the *ggt* gene. Another 14 isolates, which included seven with high asparaginase activity (range, 1.198–0.779 mM) and seven with low asparaginase activity (range, 0.322–0.185 mM), were used to compare the promoter region of the *ansB* gene. As indicated in Figure 3a, even though there was high diversity in the promoter region of the *ggt* gene between isolates, no specific polymorphism was related to either high or low γ-glutamyltranspeptidase activity.

Comparison between isolates of the promoter regions of the *ansB* gene is shown in Figure 3b. A 161 bp insertion was observed in TS1531, which had low asparaginase activity. Asparaginase of *H. pylori* is known to be a periplasmic asparaginase and to possess a signal peptide in the N-terminal region to be secreted in the periplasm (10). The insertion observed in TS1531 contained the translation start site of the secreted form of asparaginase. Specific polymorphism related to either high or low activity of asparaginase was not observed in the promoter region of the *ansB* gene.

Interleukin-8 production in AGS cells infected by *Helicobacter pylori* and mutant strains

AGS cells were infected with either *H. pylori* ATCC700392 wild-type, the Δ*ggt* strain, Δ*ansB* strain or Δ*ggt*/*ansB* strain and IL-8 production measured by ELISA 18 hr after induction of infection. As shown in Figure 4a, IL-8 production by infection of the Δ*ggt* strain (mean ± SD, 576 ± 3 pg/mL) was significantly lower than that by wild-type infection (1177 ± 17 pg/mL, $P < 0.05$). IL-8 production by Δ*ansB* infection (1140 ± 44 pg/mL) was similar to that by wild-type infection. Infection by the double-knockout strain Δ*ggt*/*ansB* led to the same level of IL-8 production (792 ± 48 pg/mL) as did infection by the Δ*ggt* strain. When glutamine was supplemented during wild-type strain infection, IL-8 production was significantly reduced (from 1177 ± 17 to 785 ± 87 pg/mL, $P < 0.05$), whereas no reduction was observed in infection by the Δ*ggt* strain (from 576 ± to 641 ± 45 pg/mL). IL-8 production was not changed by asparagine supplementation in any strain. Addition of both glutamine and asparagine led to IL-8 production similar to that seen after addition of glutamine alone in all strains.

Several glutamine concentrations (from 5–50 mM) were tested during infection by the wild-type and Δ*ggt* strains (Fig. 4b). Addition of 5 mM glutamine significantly reduced IL-8 production in wild-type strain infection (from 2478 to 1447 pg/mL, $P < 0.05$). When the concentration of glutamine was increased to 20 mM, the difference in IL-8 production between wild-type and Δ*ggt* strain infections was diminished. IL-8 production was significantly reduced when glutathione was added during wild-type strain infection (from 3411 to 1822 pg/mL, $P < 0.05$), whereas this reduction was not observed in Δ*ggt* strain infection (Fig. 4c).

DISCUSSION

The importance of γ-glutamyltranspeptidase and asparaginase in the pathogenesis of *H. pylori* infection has been described in both *in vitro* and *in vivo* studies of *H. pylori*

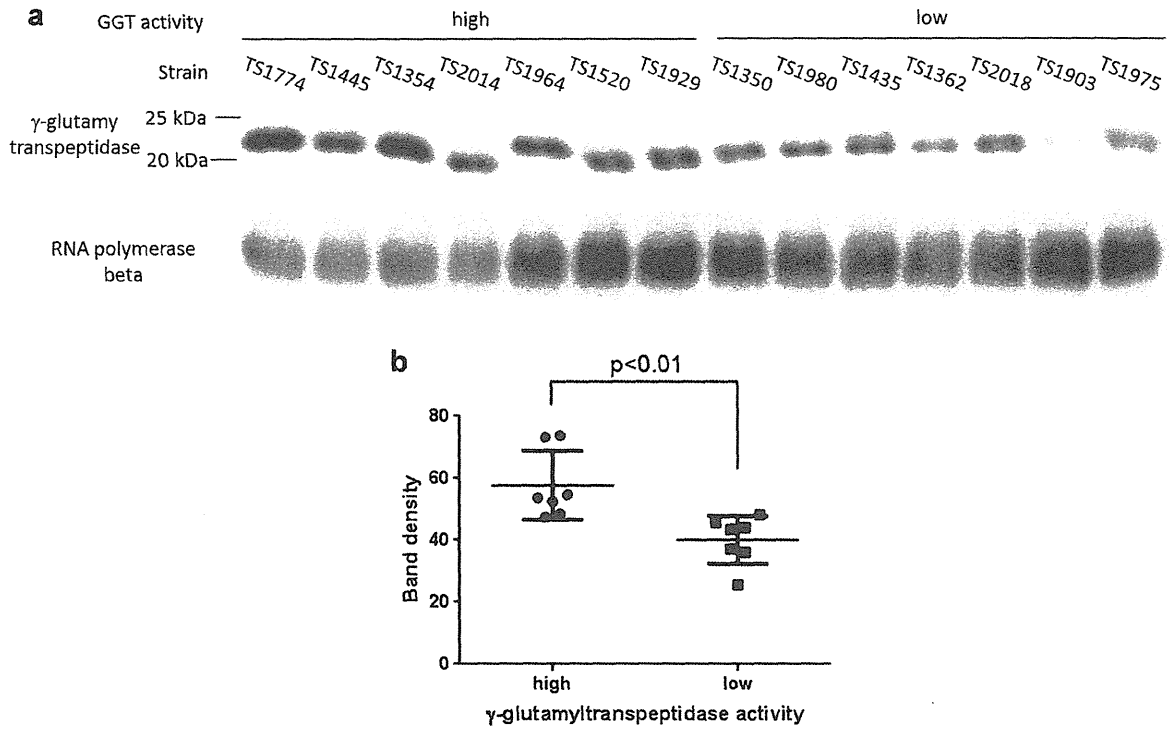

Fig. 2. Expression of γ-glutamyltranspeptidase in 14 clinical *H. pylori* isolates, which include seven isolates with high γ-glutamyltranspeptidase activity and seven with low γ-glutamyltranspeptidase activity. (a) γ-glutamyltranspeptidase expression was examined by western blot analysis. (b) Band densities were measured by ImageJ 1.45s and compared between isolates with high and low activity.

infection; however, there have been few assessments of the activities of these deamidases in clinical *H. pylori* isolates. In this study, we compared the activities of deamidases in clinical isolates from patients with different gastro-intestinal diseases and found that γ-glutamyltranspeptidase activities in *H. pylori* isolated from patients with gastric cancer were significantly higher than in that from patients with duodenal ulcer sand chronic gastritis. We also analyzed γ-glutamyltranspeptidase expression in clinical isolates and demonstrated strong expression of γ-glutamyltranspeptidase in some isolates; this represented high γ-glutamyltranspeptidase activities. However, because some isolates with high γ-glutamyltranspeptidase activities represented moderate γ-glutamyltranspeptidase expression, high γ-glutamyltranspeptidase activities may be caused by other factors such as protein stability and localization. We compared the promoter sequence of the *ggt* gene in the clinical isolates and found no significant polymorphism related to high or low activities of γ-glutamyltranspeptidase. The mechanism of high γ-glutamyltranspeptidase activity requires further investigation. Previous reports have shown higher γ-glutamyltranspeptidase activities of *H. pylori* isolates from patients with peptic ulcers than in those from patients with non-ulcer-related dyspepsia (18). In this study, the activities of γ-glutamyltranspeptidase were not significantly different between patients with peptic ulcers and those with chronic gastritis. Since non-ulcer dyspepsia is not equivalent to chronic gastritis, these two studies cannot simply be compared. However, there was a wide range of γ-glutamyltranspeptidase activity in the strains from patients with gastric ulcers and some of these strains had γ-glutamyltranspeptidase activity that was as high as that observed in the strains from patients with gastric cancer.

Using both gastric and non-gastric cells, Scotti *et al.* showed that asparaginase inhibits the cell cycle (23). We have previously demonstrated the cytotoxic activity of asparaginase against a histiocytic lymphoma cell line (13). In this study we found that the activities of asparaginase in *H. pylori* isolates from patients with gastric cancer ranged widely compared with those from other diseases and, although high, were not significantly higher than those from other diseases. An insertion sequence was observed in the *ansB* gene of strain TS1531, which had low asparaginase activity, and this sequence was inserted into a signal peptide that leads AnsB protein to the periplasm. Therefore, the low asparaginase activity in this strain

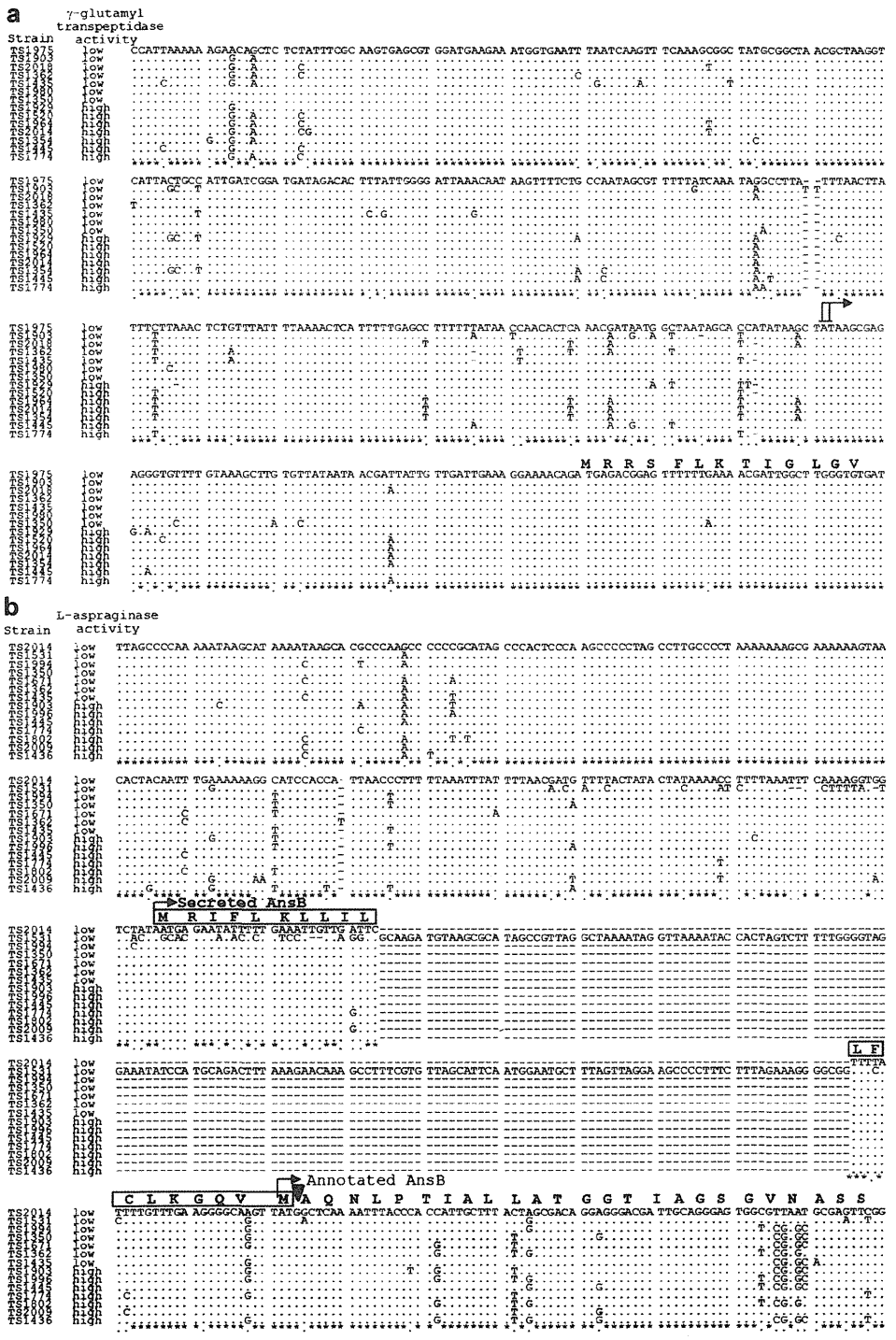

Fig. 3. Alignment of the promoter sequences of (a) the *ggt* gene and (b) *ansB* gene in clinical *H. pylori* isolates. (a) Seven clinical isolates with high γ-glutamyltranspeptidase activity and seven with low γ-glutamyltranspeptidase activity. Arrows indicate transcriptional start points identified in a previous study (21). Translational amino acids are shown above the alignment sequences. (b) Seven clinical isolates with high asparaginase activity and seven with low asparaginase activity. Translational amino acids are shown above the alignment sequences. The predicted signal peptide and cleavage point of AnsB protein, which possesses a signal peptide in the N-terminal region to be secreted in the periplasm, are marked by a box and a black inverted triangle, respectively.

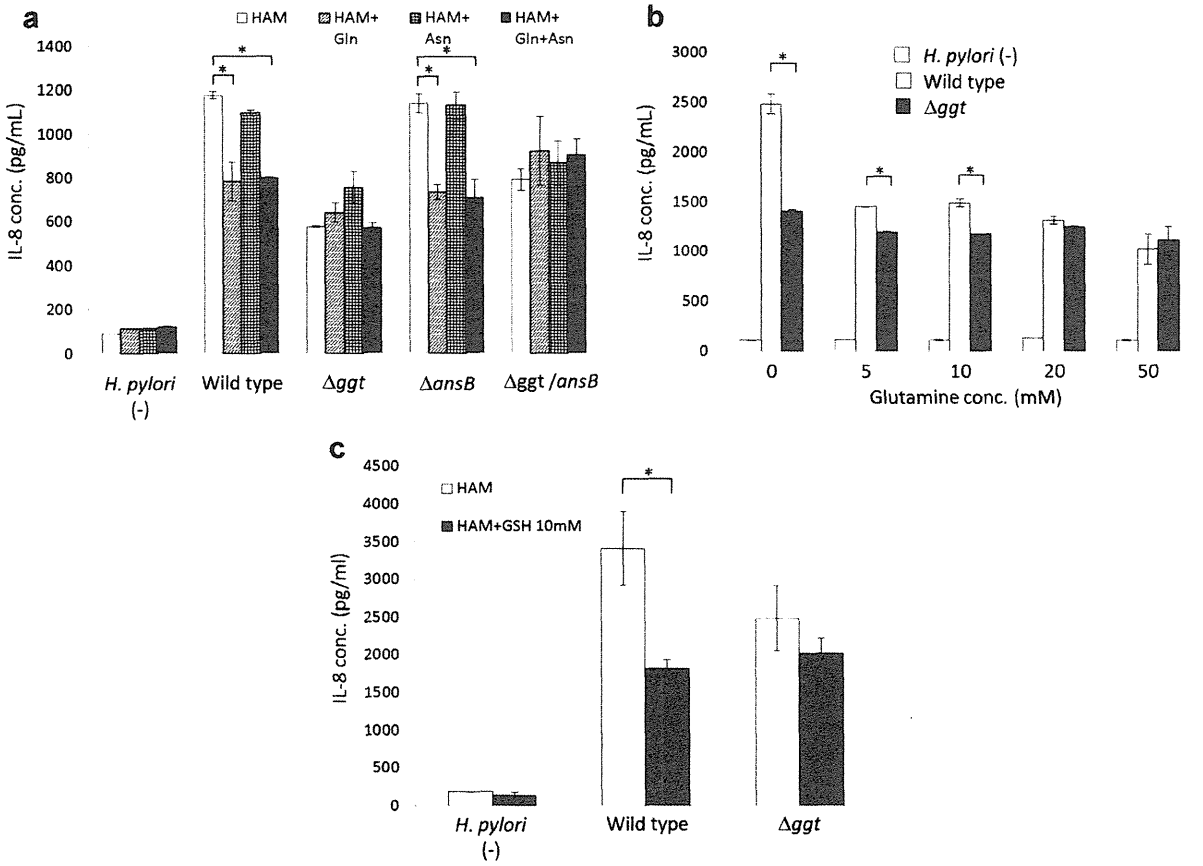

Fig. 4. Induction of IL-8)in AGS cells infected by *H. pylori* wild-type and mutant strains. (a) AGS cells were infected by the ATCC700392 wild-type, Δ*ggt*, Δ*ansB* and Δ*ggt*/*ansB* strains. During infection, 50 mM glutamine, asparagine, or both amino acids were added to the medium. After 18 hr incubation, supernatants was analyzed by ELISA to measure IL-8 concentration (pg/mL). (b) AGS cells were infected by the ATCC700392 wild-type strain and Δ*ggt* strain, respectively. During infection, 5, 10, 20 or 50 mM glutamine was added to the medium. Measurement of IL-8 was performed after 18 hr incubation. (c) AGS cells were infected by the ATCC700392 wild-type and Δ*ggt* strains. During infection, 10 mM glutathione was added to the medium. Measurement of IL-8 was performed after 18 hr incubation. *, $P < 0.05$).

could have been attributable to this insertion. However, because this insertion was not observed in the other strains, which also had low asparaginase activity, another mechanism must be involved in the difference in asparaginase activities between strains.

The mechanisms by which these deamidases contribute to the development of gastric cancer are controversial. Chronic inflammation of gastric cells caused by *H. pylori* infection is known to be a trigger of gastric cancer and it has been proposed that IL-8 contributes to chronic inflammation and cancer. We investigated the proinflammatory cytokine response by measuring the IL-8 production induced by *H. pylori* infection *in vitro* and found that the inflammatory response was significantly reduced by *ggt* gene knockout but not by *ansB* gene knockout. Moreover, IL-8 induction was significantly reduced by the addition of glutamine. Several roles of γ-glutamyltranspeptidase and asparaginase in the pathogenesis of *H. pylori* infection have been suggested; one possible route is the depletion of glutamine and asparagine caused by γ-glutamyltranspeptidase and asparaginase, respectively (10, 16, 17). However, we demonstrated in this study that depletion of asparagine by asparaginase contributed little to induction of the inflammatory response. This result corresponds to the findings of a previous study, which found that AnsB protein is not cytotoxic to gastric cell lines (13). Taken together, the depletion of glutamine, but not of asparagine, caused by high γ-glutamyltranspeptidase activity could be responsible for the strong inflammatory response caused by *H. pylori* infection. This is consistent with the results of this study, which demonstrated

significantly high γ-glutamyltranspeptidase activities in clinical isolates from patients with gastric cancer. Therefore, infection with *H. pylori* strains that possess high γ-glutamyltranspeptidase activity would increase the risk of developing gastric cancer because of depletion of glutamine in gastric cells.

Ammonia has been demonstrated to induce cell death in an *in vitro H. pylori* infection assay (24) and Leduc *et al.* demonstrated the significant role of toxic ammonia produced by deamidases in the pathogenesis of *H. pylori* (10). We measured the concentrations of ammonia in culture supernatants and found no significant difference between the wild-type strain (2.99 mM) and several knockout strains (Δ*ggt*, 2.49 mM; Δ*ansB*, 2.55 mM; Fig. S1). Moreover, ammonia concentrations increased 2.8-fold (8.35 mM) and 2.0-fold (5.94 mM) with the addition of glutamine and asparagine, respectively, when cells were infected by *H. pylori* wild-type strain (Fig. S1), whereas IL-8 induction was decreased when glutamine was added. Therefore, toxic ammonia may not contribute substantially to inflammatory responses to *H. pylori* infection. The increase in oxidative cell damage caused by hydrogen peroxide, which is produced by the degradation of glutathione by γ-glutamyltranspeptidase, has also been suggested as a mechanism for γ-glutamyltranspeptidase-related *H. pylori* pathogenicity (18, 19). However, we observed a significant reduction in IL-8 production after adding glutathione during wild-type strain infection; however, we did not observe this in Δ*ggt* strain infection. These observations suggest that degradation of glutathione is not responsible for the inflammatory response. Taken together, depletion of glutamine could be mainly responsible for the inflammatory response caused by high γ-glutamyltranspeptidase activity of *H. pylori*. The beneficial effects of supplemental glutamine have been reported in animal models (25, 26); however, further analysis is needed to elucidate whether supplemental glutamine could reduce the risk of developing gastric cancer caused by chronic *H. pylori* infection.

In conclusion, in this study we measured γ-glutamyltranspeptidase and asparaginase activities in *H. pylori* strains from patients gastrointestinal-related disease and demonstrated significantly higher γ-glutamyltranspeptidase activities in *H. pylori* strains from patients with gastric cancer than in those from patients with chronic gastritis and duodenal ulcers. We suggest that the inflammatory response caused by γ-glutamyltranspeptidase activity of *H. pylori* is attributable to depletion of glutamine. These data suggest a significant role of γ-glutamyltranspeptidase in the chronic inflammation caused by *H. pylori* infection.

ACKNOWLEDGMENTS

We thank Drs. Norihisa Noguchi, Takashi Kawai and Masanori Sasatsu for providing the *H. pylori* isolates used in this study. This study was supported by a Grant-in-Aid for Scientific Research (C) from the Japan Society for the Promotion of Science (No. 22590410) and a grant from the Ministry of Health, Labour and Welfare of Japan (H21-Shinkou-Ippan-008).

DISCLOSURE

The authors declare no conflicts of interest.

REFERENCES

1. Warren J.R., Marshall B. (1983) Unidentified curved bacilli on gastric epithelium in active chronic gastritis. *Lancet* **1**: 1273–5.
2. Chan F.K.L. (2002) Eradication of *Helicobacter pylori* and risk of peptic ulcers in patients starting long-term treatment with non-steroidal anti-inflammatory drugs: a randomised trial. *Lancet* **359**: 9.
3. Parsonnet J., Friedman G.D., Vandersteen D.P., Chang Y., Vogelman J.H., Orentreich N., Sibley R.K. (1991) *Helicobacter pylori* infection and the risk of gastric carcinoma. *N Engl J Med* **325**: 1127–31.
4. Miwa H., Go M.F., Sato N. (2002) *H. pylori* and gastric cancer: the Asian enigma. *Am J Gastroenterol* **97**: 1106–12.
5. Hatakeyama M. (2009) *Helicobacter pylori* and gastric carcinogenesis. *J Gastroenterol* **44**: 239–48.
6. Cover T.L. (2005) *Helicobacter pylori* VacA, a paradigm for toxin multifunctionality. *Nat Rev Microbiol* **3**: 320.
7. Basso D., Zambon C.-F., Letley D., Stranges A., Marchet A., Rhead J., Schiavon S., Guariso G., Ceroti M., Nitti D., Rugge M., Plebani M., Atherton J. (2008) Clinical relevance of *Helicobacter pylori* cagA and vacA gene polymorphisms. *Gastroenterology* **135**: 91–9.
8. Covacci A., Telford J.L., Giudice G.D., Parsonnet J., Rappuoli R. (1999) *Helicobacter pylori* virulence and genetic geography. *Science* **284**: 1328–33.
9. Argent R.H., Hale J.L., El-Omar E.M., Atherton J.C. (2008) Differences in *Helicobacter pylori* CagA tyrosine phosphorylation motif patterns between western and east Asian strains, and influences on interleukin-8 secretion. *J Med Microbiol* **57**: 1062–7.
10. Leduc D., Gallaud J., Stingl K., De Reuse H. (2010) Coupled amino acid deamidase-transport systems essential for *Helicobacter pylori* colonization. *Infect Immun* **78**: 2782–92.
11. Shibayama K., Kamachi K., Nagata N., Yagi T., Nada T., Doi Y., Shibata N., Yokoyama K., Yamane K., Kato H., Iinuma Y., Arakawa Y. (2003) A novel apoptosis-inducing protein from *Helicobacter pylori*. *Mol Microbiol* **47**: 443–51.
12. Schmees C., Prinz C., Treptau T., Rad R., Hengst L., Voland P., Bauer S., Brenner L., Schmid R., Gerhard M. (2007) Inhibition of T-cell proliferation by *Helicobacter pylori* gamma-glutamyl transpeptidase. *Gastroenterology* **132**: 1820–33.
13. Shibayama K., Takeuchi H., Wachino J.-I., Mori S., Arakawa Y. (2011) Biochemical and pathophysiological characterization of *Helicobacter pylori* asparaginase. *Microbiol Immunol* **55**: 408–17.
14. Chevalier C., Thiberge J.-M., Ferrero R.L., Labigne A. (1999) Essential role of *Helicobacter pylori* γ-glutamyltranspeptidase for

the colonization of the gastric mucosa of mice. *Mol Microbiol* **31**: 1359–72.
15. Mcgovern K.J., Blanchard T.G., Gutierrez J.A., Czinn S.J., Krakowka S., Youngman P. (2001) Gamma-glutamyltransferase is a *Helicobacter pylori* virulence factor but is not essential for colonization. *Infect Immun* **69**: 4168–73.
16. Shibayama K., Wachino J.-I., Arakawa Y., Saidijam M., Rutherford N., Henderson P.J.F. (2007) Metabolism of glutamine and glutathione via gamma-glutamyltranspeptidase and glutamate transport in *Helicobacter pylori*: possible significance in the pathophysiology of the organism. *Mol Microbiol* **64**: 396–406.
17. Stark R.M., Suleiman M.S., Hassan I.J., Greenman J., Millar M.R. (1997) Amino acid utilisation and deamination of glutamine and asparagine by *Helicobacter pylori*. *J Med Microbiol* **46**: 793–800.
18. Gong M., Ling S.S.M., Lui S.Y., Yeoh K.G., Ho B. (2010) *Helicobacter pylori* γ-glutamyl transpeptidase is a pathogenic factor in the development of peptic ulcer disease. *Gastroenterology* **139**: 564–73.
19. Flahou B., Haesebrouck F., Chiers K., Van Deun K., De Smet L., Devreese B., Vandenberghe I., Favoreel H., Smet A., Pasmans F., D'herde K., Ducatelle R. (2011) Gastric epithelial cell death caused by *Helicobacter suis* and *Helicobacter pylori* γ-glutamyl transpeptidase is mainly glutathione degradation-dependent. *Cell Microbiol* **13**: 1933–55.
20. Rimbara E., Noguchi N., Tanabe M., Kawai T., Matsumoto Y., Sasatsu M. (2005) Susceptibilities to clarithromycin, amoxycillin and metronidazole of *Helicobacter pylori* isolates from the antrum and corpus in Tokyo, Japan, 1995–2001. *Clin Microbiol Infect* **11**: 307–11.
21. Wachino J., Shibayama K., Suzuki S., Yamane K., Mori S., Arakawa Y. (2010) Profile of expression of *Helicobacter pylori* gamma-glutamyltranspeptidase. *Helicobacter* **15**: 184–92.
22. Schneider C.A., Rasband W.S., Eliceiri K.W. (2012) NIH image to ImageJ: 25 years of image analysis. *Nat Methods* **9**: 671–5.
23. Scotti C., Sommi P., Pasquetto M., Cappelletti D., Stivala S., Mignosi P., Savio M., Chiarelli L., Valentini G., Bolanos Garcia V., Merrell D., Franchini S., Verona M., Bolis C., Solcia E., Manca R., Franciotta D., Casasco A., Filipazzi P., Zardini E., Vannini V. (2010) Cell-cycle inhibition by *Helicobacter pylori* L-asparaginase. *PLoS ONE* **5**: e13892.
24. Nakamura E., Hagen S.J. (2002) Role of glutamine and arginase in protection against ammonia-induced cell death in gastric epithelial cells. *Am J Physiol Gastrointest Liver Physiol* **283**: G1264–75.
25. Okabe S., Takeuchi K., Takata Y., Naganuma T., Takagi K. (1976) Effects of L-glutamine on various gastric lesions in rats and guinea pigs. *Digestion* **14**: 325–31.
26. Hagen S.J., Ohtani M., Zhou J.-R., Taylor N.S., Rickman B.H., Blackburn G.L., Fox J.G. (2009) Inflammation and foveolar hyperplasia are reduced by supplemental dietary glutamine during *Helicobacter pylori* infection in mice. *J Nutr* **139**: 912–8.

SUPPORTING INFORMATION

Additional supporting information may be found in the online version of this article on the publisher's web-site.

Fig. S1. Production of ammonia in culture supernatants of *H. pylori*-infected AGS cells. AGS cells were infected by the ATCC700392 wild-type, Δ*ggt*, Δ*ansB* and Δ*ggt*/*ansB* strains. During infection, 50 mM glutamine or asparagine was added to the medium.

genome
Journals.ASM.org

Draft Genome Sequence of *Helicobacter fennelliae* Strain MRY12-0050, Isolated from a Bacteremia Patient

Emiko Rimbara,[a] Mari Matsui,[a] Shigetarou Mori,[a] Satowa Suzuki,[a] Masato Suzuki,[a] Hyun Kim,[a] Tsuyoshi Sekizuka,[b] Makoto Kuroda,[b] Keigo Shibayama[a]

Department of Bacteriology II, National Institute of Infectious Diseases, Musashimurayama-shi, Tokyo, Japan[a]; Laboratory of Bacterial Genomics, Pathogen Genomics Center, National Institute of Infectious Diseases, Shinjuku-ku, Tokyo, Japan[b]

***Helicobacter fennelliae*, a human enterohepatic pathogen, causes bacteremia and colitis. We isolated *H. fennelliae* strain MRY12-0050 from a female patient; this strain was isolated from 2 other patients from the same hospital during the same period, suggesting human-to-human transmission. This is the first report of an *H. fennelliae* genome sequence.**

Received 3 July 2013 **Accepted** 11 July 2013 **Published** 8 August 2013

Citation Rimbara E, Matsui M, Mori S, Suzuki S, Suzuki M, Kim H, Sekizuka T, Kuroda M, Shibayama K. 2013. Draft genome sequence of *Helicobacter fennelliae* strain MRY12-0050, isolated from a bacteremia patient. Genome Announc. 1(4):e00512-13. doi:10.1128/genomeA.00512-13.

Address correspondence to Emiko Rimbara, rimbara@nih.go.jp.

Helicobacter species are Gram-negative, spiral bacteria that are categorized into 2 groups, (i) gastric helicobacters and (ii) enterohepatic helicobacters. *Helicobacter pylori* is a major gastric *Helicobacter*, and the genome sequences of several gastric *Helicobacter* strains have been analyzed so far. On the other hand, analyses of genomic sequences for enterohepatic helicobacters have been limited. *H. fennelliae* is an enterohepatic *Helicobacter* that causes bacteremia mainly in immunocompromised hosts (1–3). In this study, *H. fennelliae* strain MRY12-0050 was isolated from the blood of a female patient with non-Hodgkin lymphoma. At first, the strain was misidentified as *H. cinaedi* because the strains have similar morphologies. It was later identified as *H. fennelliae* by sequencing of both the 16S rRNA and 23S rRNA genes. *H. fennelliae* was isolated from 2 other patients from the same hospital ward. Pulsed-field gel electrophoresis (PGFE) of 3 isolates showed the same PFGE pattern between isolates, suggesting human-to-human transmission (4). Since genome-sequencing data for *H. fennelliae* have not yet been reported, we herein describe a draft genome sequence for *H. fennelliae* MRY 12-0050, which causes nosocomial infection.

H. fennelliae was cultured in brucella agar (Becton Dickinson, NJ) containing 5% horse blood under microaerobic conditions with hydrogen, which was provided by the gas replacement method by using an anaerobic gas mixture (i.e., H_2, 10%; CO_2, 10%; and N_2, 80%). Genomic DNA was prepared, and a Roche 454 Life Sciences genome sequencer junior system was used to generate DNA sequences at 32× coverage. The same genomic DNA was analyzed by the Illumina MiSeq system paired-end sequences, and the resulting sequence represents 127× coverage. Sequences obtained by using the Roche 454 were assembled using Newbler Assembler v2.7, whereas sequences obtained by using the Illumina MiSeq were assembled with Geneious. The assembled sequences were merged by using Geneious to generate 49 contigs. The contig N_{50} was approximately 157 kb in length, and the largest contig assembled was approximately 300 kb. Finally, the DNA sequences were annotated by using the RAST (Rapid Annotation using Subsystem Technology) server (5).

The whole genome is 2.15 Mb in size, has a G+C content of 37.9%, and contains 2,507 genes (2,467 protein-coding genes and 40 structural RNAs). RAST annotation showed that *H. cinaedi* strain CCUG 18818 (score 502), *H. hepaticus* strain ATCC 51449 (score 456), and *H. canadensis* strain MIT 98-5491 (score 444) are the closest neighbors of *H. fennelliae* MRY12-0050. Although *H. cinaedi* and *H. hepaticus* have been known to express cytolethal distending toxin (CDT), which causes DNA damage to target cells, a CDT cluster was not identified in *H. fennelliae* MRY12-0050. Because both *H. cinaedi* and *H. fennelliae* are likely to cause a nosocomial infection and bacteremia in humans, further analyses are needed to elucidate the pathogenic factor in *H. fennelliae*.

Nucleotide sequence accession numbers. This whole-genome shotgun project has been deposited at DDBJ/EMBL/GenBank under the accession no. BASD00000000. The version described in this paper is the first version, BASD01000000.

ACKNOWLEDGMENTS

We thank Yuko Sasaki, Kumiko Kai, Yoshie Taki, and Yumiko Yoshimura for their technical assistance. We also thank Shunji Takahashi, Satoshi Yamamoto, and Masaya Mukai for providing bacterial isolates and clinical information.

This study was supported by a Grant-in-Aid for Young Scientists (B) from the Japan Society for the Promotion of Science (no. 25860105) and a grant from the Ministry of Health, Labor, and Welfare of Japan (H24-Shinkou-Ippan-010).

REFERENCES

1. **Burnens AP, Stanley J, Schaad UB, Nicolet J.** 1993. Novel campylobacter-like organism resembling *Helicobacter fennelliae* isolated from a boy with gastroenteritis and from dogs. J. Clin. Microbiol. **31**:1916–1917.
2. **Hsueh PR, Teng LJ, Hung CC, Chen YC, Yang PC, Ho SW, Luh KT.** 1999. Septic shock due to *Helicobacter fennelliae* in a non-human immunodeficiency virus-infected heterosexual patient. J. Clin. Microbiol. **37**: 2084–2086.
3. **Smuts HE, Lastovica AJ.** 2011. Molecular characterization of the 16S rRNA

gene of *Helicobacter fennelliae* Isolated from stools and blood cultures from paediatric patients in South Africa. J. Pathog. doi:10.4061/2011/217376.

4. **Rimbara E, Mori S, Kim H, Matsui M, Suzuki S, Takahashi S, Yamamoto S, Mukai M, Shibayama K.** 2013. *Helicobacter cinaedi* and *Helicobacter fennelliae* transmission in a hospital from 2008 to 2012. J. Clin. Microbiol. **51**:2439–2442.

5. **Aziz RK, Bartels D, Best AA, DeJongh M, Disz T, Edwards RA, Formsma K, Gerdes S, Glass EM, Kubal M, Meyer F, Olsen GJ, Olson R, Osterman AL, Overbeek RA, McNeil LK, Paarmann D, Paczian T, Parrello B, Pusch GD, Reich C, Stevens R, Vassieva O, Vonstein V, Wilke A, Zagnitko O.** 2008. The RAST server: rapid annotations using subsystems technology. BMC Genomics **9**:75. doi:10.1186/1471-2164-9-75.

genomeA
Journals.ASM.org

Genome Sequences of Multidrug-Resistant *Acinetobacter baumannii* Strains from Nosocomial Outbreaks in Japan

Masato Suzuki,[a] Mari Matsui,[a] Satowa Suzuki,[a] Emiko Rimbara,[a] Satomi Asai,[b] Hayato Miyachi,[b] Tohru Takata,[c] Yoichi Hiraki,[d] Fumio Kawano,[e] Keigo Shibayama[a]

Department of Bacteriology II, National Institute of Infectious Diseases, Musashimurayama, Tokyo, Japan[a]; Department of Laboratory Medicine, Tokai University School of Medicine, Isehara, Kanagawa, Japan[b]; Department of Infection Control, Fukuoka University Hospital, Nanakuma, Jonan-ku, Fukuoka, Japan[c]; Department of Pharmacy National Hospital, Organization Kumamoto Medical Center, Ninomaru, Chuo-ku, Kumamoto, Japan[d]; Department of Hematology, National Hospital, Organization Kumamoto Medical Center, Ninomaru, Chuo-ku, Kumamoto, Japan[e]

***Acinetobacter baumannii* has emerged worldwide as an important nosocomial pathogen in medical institutions. Here, we present the draft genome sequences of *A. baumannii* strains MRY09-0642, MRY10-0558, and MRY12-0277 that were isolated from nosocomial outbreaks in Japan between 2008 and 2012 and that are resistant to antimicrobial agents, including carbapenems, fluoroquinolones, and aminoglycosides.**

Received 4 June 2013 **Accepted** 13 June 2013 **Published** 18 July 2013

Citation Suzuki M, Matsui M, Suzuki S, Rimbara E, Asai S, Miyachi H, Takata T, Hiraki Y, Kawano F, Shibayama K. 2013. Genome sequences of multidrug-resistant *Acinetobacter baumannii* strains from nosocomial outbreaks in Japan. Genome Announc. 1(4):e00476-13. doi:10.1128/genomeA.00476-13.

Address correspondence to Masato Suzuki, suzuki-m@nih.go.jp.

Acinetobacter baumannii often causes infections in hospitalized immunocompromised patients (1). *A. baumannii* strains belonging to international clone II (IC2)/sequence type 2 (ST2), the most prevalent epidemic lineage, are associated with multidrug resistance and often cause nosocomial outbreaks (2). Since 2000, carbapenem-resistant and multidrug-resistant *A. baumannii* strains have emerged and their prevalence has increased worldwide. In some countries, carbapenem-resistant strains have reached a prevalence of >50%, becoming a serious public health threat (3). According to national surveillance data from Japan Nosocomial Infections Surveillance (JANIS) conducted by the Ministry of Health, Labour and Welfare (http://www.nih-janis.jp/english/), carbapenem resistance among *Acinetobacter* spp. in Japan remains much lower than in other countries (approximately 2% of imipenem resistance in Japan in 2012) (S. Suzuki, unpublished data). However, the prevalence tends to increase gradually, and nosocomial outbreaks of *A. baumannii* IC2 infections have occasionally occurred in Japan.

To date, whole-genome sequences of *A. baumannii* strains isolated in Japan have not been available in GenBank. In this report, we announce the availability of the draft genome sequences of *A. baumannii* MRY09-0642, MRY10-0558, and MRY12-0277, which caused nosocomial outbreaks in geographically different medical institutions in Japan in 2008, 2010, and 2012, respectively. These isolates were classified as IC2 by multilocus sequence typing (4), whereas they showed distinct ApaI fragment patterns in pulsed-field gel electrophoresis. Whole-genome shotgun (WGS) sequencing of the *A. baumannii* strains was performed using the Roche 454 pyrosequencing platform (500-bp insert size). Reads were assembled with Newbler assembler version 2.3 (Roche), using *A. baumannii* Taiwanese strain MDR-TJ (5) as the reference.

The draft genome sequences of *A. baumannii* MRY09-0642, MRY10-0558, and MRY12-0277 consist of 147, 77, and 106 contigs, respectively, yielding total sequences for each strain of 3,746,543, 3,782,742, and 3,829,745 bp, with N_{50} contig sizes of 64,650, 164,570, and 91,207 bp, respectively. Their mean G+C content is 39.0% ± 0.1%. A total of 3,645, 3,604, and 3,735 coding genes for MRY09-0642, MRY10-0558, and MRY12-0277, respectively, were detected by the RAST server (http://rast.nmpdr.org) (6). Acquired antimicrobial resistance genes in the WGS data were identified using a Web-based tool, ResFinder version 1.3 (http://cge.cbs.dtu.dk/services/ResFinder/) (7). *A. baumannii* MRY09-0642, MRY10-0558, and MRY12-0277 carry OXA-51-like β-lactamase genes, which predominantly confer carbapenem resistance in *A. baumannii* (8), found as $bla_{\text{OXA-82}}$ in contig 00088, $bla_{\text{OXA-254}}$ in contig 00034, and $bla_{\text{OXA-66}}$ in contig 00056, respectively.

A more-detailed report of the drug resistance and virulence phenotypes of these three *A. baumannii* strains will be included in a future publication. Access to these genome sequences and their comparative analyses with other epidemic and nonepidemic strains will facilitate additional comprehensive bioinformatics and phylogenetic analyses, thus expanding our understanding of the global public health problem caused by this nosocomial pathogen.

Nucleotide sequence accession numbers. These WGS projects have been deposited at DDBJ/EMBL/GenBank under the accession no. BASA00000000, BASB00000000, and BASC00000000. The versions described in this report are the first versions, accession no. BASA01000000, BASB01000000, and BASC01000000 for *A. baumannii* strains MRY09-0642, MRY10-0558, and MRY12-0277, respectively.

ACKNOWLEDGMENTS

We thank Yuko Sasaki, Kumiko Kai, Yoshie Taki, and Yumiko Yoshimura for technical assistance. We are grateful to all of the participating medical institutions for providing bacterial isolates and clinical information.

This work is supported by a Grant-in-Aid for Young Scientists (A)

(25713017) from the Ministry of Education, Culture, Sports, Science and Technology, Japan, and H24-Shinkou-Ippan-010 from the Ministry of Health, Labour and Welfare, Japan.

REFERENCES

1. **Dijkshoorn L, Nemec A, Seifert H.** 2007. An increasing threat in hospitals: multidrug-resistant *Acinetobacter baumannii*. Nat. Rev. Microbiol. 5:939–951.
2. **Diancourt L, Passet V, Nemec A, Dijkshoorn L, Brisse S.** 2010. The population structure of *Acinetobacter baumannii*: expanding multiresistant clones from an ancestral susceptible genetic pool. PLoS One 5:e10034. doi: 10.1371/journal.pone.0010034.
3. **Laxminarayan R, Klugman KP.** 2011. Communicating trends in resistance using a drug resistance index. BMJ Open 1:e000135. doi:10.1136/bmjopen -2011-000135.
4. **Matsui M, Suzuki S, Suzuki M, Arakawa Y, Shibayama K.** 2013. Rapid discrimination of *Acinetobacter baumannii* international clone II lineage by pyrosequencing SNP analyses of bla_{OXA} 51-like genes. J. Microbiol. Methods 94:121–124.
5. **Gao F, Wang Y, Liu YJ, Wu XM, Lv X, Gan YR, Song SD, Huang H.** 2011. Genome sequence of *Acinetobacter baumannii* MDR-TJ. J. Bacteriol. 193:2365–2366.
6. **Aziz RK, Bartels D, Best AA, DeJongh M, Disz T, Edwards RA, Formsma K, Gerdes S, Glass EM, Kubal M, Meyer F, Olsen GJ, Olson R, Osterman AL, Overbeek RA, McNeil LK, Paarmann D, Paczian T, Parrello B, Pusch GD, Reich C, Stevens R, Vassieva O, Vonstein V, Wilke A, Zagnitko O.** 2008. The RAST server: rapid annotations using subsystems technology. BMC Genomics 9:75. doi:10.1186/1471-2164-9-75.
7. **Zankari E, Hasman H, Cosentino S, Vestergaard M, Rasmussen S, Lund O, Aarestrup FM, Larsen MV.** 2012. Identification of acquired antimicrobial resistance genes. J. Antimicrob. Chemother. 67:2640–2644.
8. **Lee JH, Choi CH, Kang HY, Lee JY, Kim J, Lee YC, Seol SY, Cho DT, Kim KW, Song do Y, Lee JC.** 2007. Differences in phenotypic and genotypic traits against antimicrobial agents between *Acinetobacter baumannii* and *Acinetobacter* genomic species 13TU. J. Antimicrob. Chemother. 59: 633–639.

Journal of Microbiological Methods 94 (2013) 121–124

Contents lists available at SciVerse ScienceDirect

Journal of Microbiological Methods

journal homepage: www.elsevier.com/locate/jmicmeth

Note

Rapid discrimination of *Acinetobacter baumannii* international clone II lineage by pyrosequencing SNP analyses of $bla_{OXA\text{-}51\text{-}like}$ genes

Mari Matsui [a,*], Satowa Suzuki [a], Masato Suzuki [a], Yoshichika Arakawa [b], Keigo Shibayama [a]

[a] Department of Bacteriology II, National Institute of Infectious Diseases, Tokyo, Japan
[b] Department of Bacteriology, Nagoya University Graduate School of Medicine, Nagoya Japan

ARTICLE INFO

Article history:
Received 1 March 2013
Received in revised form 21 May 2013
Accepted 21 May 2013
Available online 26 May 2013

Keywords:
Acinetobacter baumannii
$bla_{OXA\text{-}51\text{-}like}$
Pyrosequence

ABSTRACT

We found that *Acinetobacter baumannii* international clone II generally possesses unique GTA sequence at nucleotide positions 106–108 in the $bla_{OXA\text{-}51\text{-}like}$ genes. We exploited this to develop an easy and rapid method for discrimination of international clone II from other *A. baumannii* by employing pyrosequencing analyses of single nucleotide polymorphisms.

Acinetobacter species often cause infections in hospitalized immunocompromised patients (Peleg et al., 2008). In *Acinetobacter baumannii*, epidemic type lineages, international clone I and II have caused outbreaks in clinical settings worldwide. Others, mainly from sporadic cases, are regarded as non-epidemic types. Today the international clone II lineage is the most prevalent epidemic type; it is associated with multidrug-resistance and often causes nosocomial infections (Diancourt et al., 2010). The prevalence of this lineage is of concern from the viewpoint of healthcare safety. The type of lineage can be identified by several genotyping methods (Dijkshoorn et al., 1996; Bartual et al., 2005; Turton et al., 2007; Diancourt et al., 2010; Higgins et al., 2010). Multilocus sequence typing (MLST) is widely used as the golden standard method for analyses of bacterial genetic lineages (Zarrilli et al., 2013). Two MLST schemes are implemented for *Acinetobacter* spp.; the international clone II corresponds to sequence type 2 (ST2) and clonal complex 92 based on the Pasteur Institute scheme and the Bartual scheme, respectively (Bartual et al., 2005; Diancourt et al., 2010). However, these genetic identification methods are relatively complex and considerably expensive. Development of an easy, rapid, and less expensive method for discrimination of the international clone II from other genetic lineages among *Acinetobacter* spp., especially *A. baumannii*, is desirable.

Pyrosequencing is a bioluminometric assay that allows rapid and high-throughput sequencing of short DNA sequences (Ronaghi et al., 1998). This technique has been used to detect nucleotide substitutions and genotypes of a variety of bacteria (Jones et al., 2009; Spuesens et al., 2010). In this study, we identified a nucleotide sequence specific for the *A. baumannii* international clone II and applied pyrosequencing of SNPs in $bla_{OXA\text{-}51\text{-}like}$ genes to rapid and simple differentiation of the international clone II from other *A. baumannii* genetic lineages. This method holds promise as a convenient approach for identifying international clone II lineage isolates.

Thirty-six *A. baumannii* isolates, displaying different pulsed-field gel electrophoresis band patterns, were used in this study. These had been isolated in 22 Japanese medical institutions between 2000 and 2011. In addition, 2 ATCC type strains of *A. baumannii* (ATCC17978 and ATCC19606) were also included. Species-level exact identification as *A. baumannii* was performed by sequencing of *rpoB* (La Scola et al., 2006) and restriction analysis of the 16S–23S rRNA intergenic spacer sequences (Dolzani et al., 1995). Genotypes of the isolates were determined by conventional MLST methods. Among 36 clinical isolates, 21 belonged to Pasteur Institute scheme ST2. They were ST92 or 7 other ST92-related STs, by the Bartual scheme; thus, the 21 isolates were verified as belonging to the international clone II lineage (Table 1). Fifteen other clinical isolates and the two ATCC type strains were classified into various STs other than the international clone II lineage by both the Pasteur Institute and Bartual schemes (Table 1).

A. baumannii carries an intrinsic OXA-51-like β-lactamase gene on the chromosome (Héritier et al., 2005). Based on differences in amino acid sequence, more than 60 variants of OXA-51-like β-lactamases have been identified among *A. baumannii* strains to date. We determined the nucleotide sequence of $bla_{OXA\text{-}51\text{-}like}$ genes of the 36 *A. baumannii* isolates, as described by Héritier et al. previously (Héritier et al., 2005). By comparing the nucleotide sequence alignments, we identified a unique

* Corresponding author at: Department of Bacteriology II, National Institute of Infectious Diseases, 4-7-1 Gakuen, Musashi-Murayama, Tokyo 208-0011, Japan. Tel.: +81 42 561 0771; fax: +81 42 561 7173.
E-mail address: m-matsui@nih.go.jp (M. Matsui).

0167-7012/$ – see front matter © 2013 Elsevier B.V. All rights reserved.
http://dx.doi.org/10.1016/j.mimet.2013.05.014

Table 1
Clinical isolates and reference strains used in this study.

	Sequence Type		$bla_{OXA-51-like}$ type	Nucleotide sequence (nt 106–108)	Number of isolates
	Pasteur Inst.	Bartual			
International clone II (n = 21)	2	92	OXA-66	GTA	6
	2	74	OXA-66	GTA	3
	2	75	OXA-66	GTA	1
	2	76	OXA-66	GTA	1
	2	138	OXA-66	GTA	1
	2	189	OXA-66	GTA	1
	2	255	OXA-66	GTA	1
	2	257	OXA-66	GTA	1
	2	92	OXA-82	GTA	4
	2	92	OXA-83	GTA	1
	2	92	OXA-254	GTA	1
Other clone types (n = 17)	1	109	OXA-69	GAC	1
	1	135	OXA-69	GAC	1
	34	79	OXA-69	GAC	1
	153	80	OXA-69	GAC	1
	148	85	OXA-85	GAC	1
	33	86	OXA-86	GAC	1
	151	83	OXA-120	GAC	1
	146	82	OXA-51	GAA	1
	145	81	OXA-65	GAA	1
	147	84	OXA-65	GAA	1
	152	458	OXA-65	GAA	1
	212	459	OXA-100	GAA	1
	149	78	OXA-104	GAA	1
	150	77	OXA-121	GAA	1
	77	112	OXA-95	GAA	ATCC17978
	52	26	OXA-98	GAA	ATCC19606
	103	87	OXA-70	AAA	1

sequence, GTA, which was conserved exclusively among the international clone II isolates, from position 106 to 108 of the gene (Table 1). The non-international clone II isolates carried either GAC, GAA, or AAA at the position (Table 1). OXA-51-like β-lactamase gene type of 15 international clone II isolates was OXA-66, which is the most common variant type among the international clone II lineage (Evans et al., 2008). The other isolates belonging to the international clone II lineage carried OXA-82, OXA-83, or a novel variant, OXA-254 (GenBank accession number AB781687) (Table 1). The bla_{OXA} genes of the non-international clone II isolates were classified into 12 different types. A phylogenetic tree of the OXA-51-like β-lactamase genes was constructed with the nucleotide sequences of $bla_{OXA-51-like}$ genes in these isolates and those previously reported with MLST data (Hamouda et al., 2010; Zander et al., 2012) by the neighbor-joining clustering algorithm and the Jukes–Cantor distance model, using BioNumetrics 7.0 software (Applied Maths, Sint-Martens-Latern, Belgium). All eight known OXA-51-like β-lactamase variants of the international clone II lineage formed a single cluster (Fig. 1), indicating that the nucleotide sequence pattern of each OXA-51-like gene correlates with the ST defined by MLST, as described previously (Hamouda et al., 2010). To further verify that the GTA sequence is specific for the international clone II lineage, we checked the sequences and MLST available on GenBank database. The results are shown in Table S1. Indeed, the GTA sequence was generally conserved among the all 40 international clone II strains checked, but found in none of the 38 non-international clone II strains. In addition, we checked the presence of the OXA-51-like gene in 55 non-*baumannii Acinetobacter* spp., which consisted of non-repetitive 21 *A. pittii*, 27 *A. nosocomialis*, and 7 other *Acinetobacter* spp., identified by sequencing of *rpoB* (La Scola et al.,

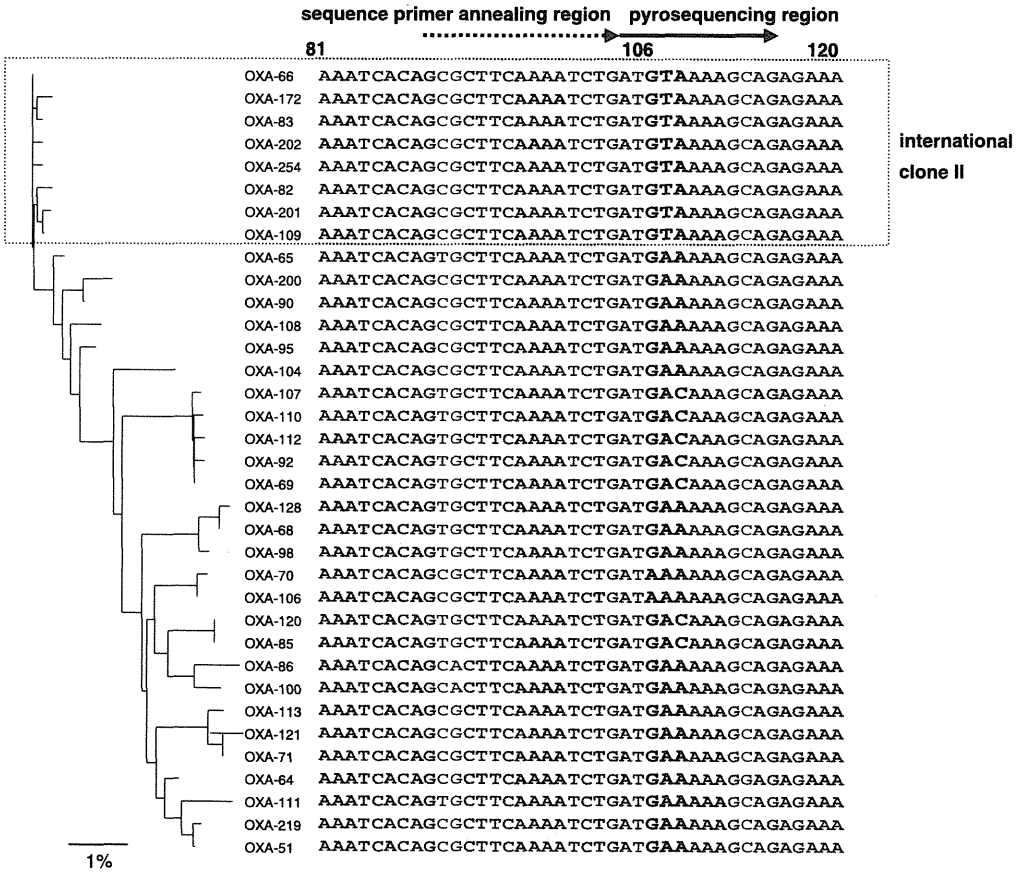

Fig. 1. Phylogenetic tree and sequence alignment of 35 $bla_{OXA-51-like}$ variants. Nucleotide sequences from position 81 to 120 are shown. Areas highlighted by gray color indicate conserved sequences. Dotted arrow indicates the sequence primer annealing region (15 bp) and solid arrow indicates the pyrosequencing region (12 bp). The unique sequence region identified as the marker for discrimination of the international clone II lineage is shown in bold.

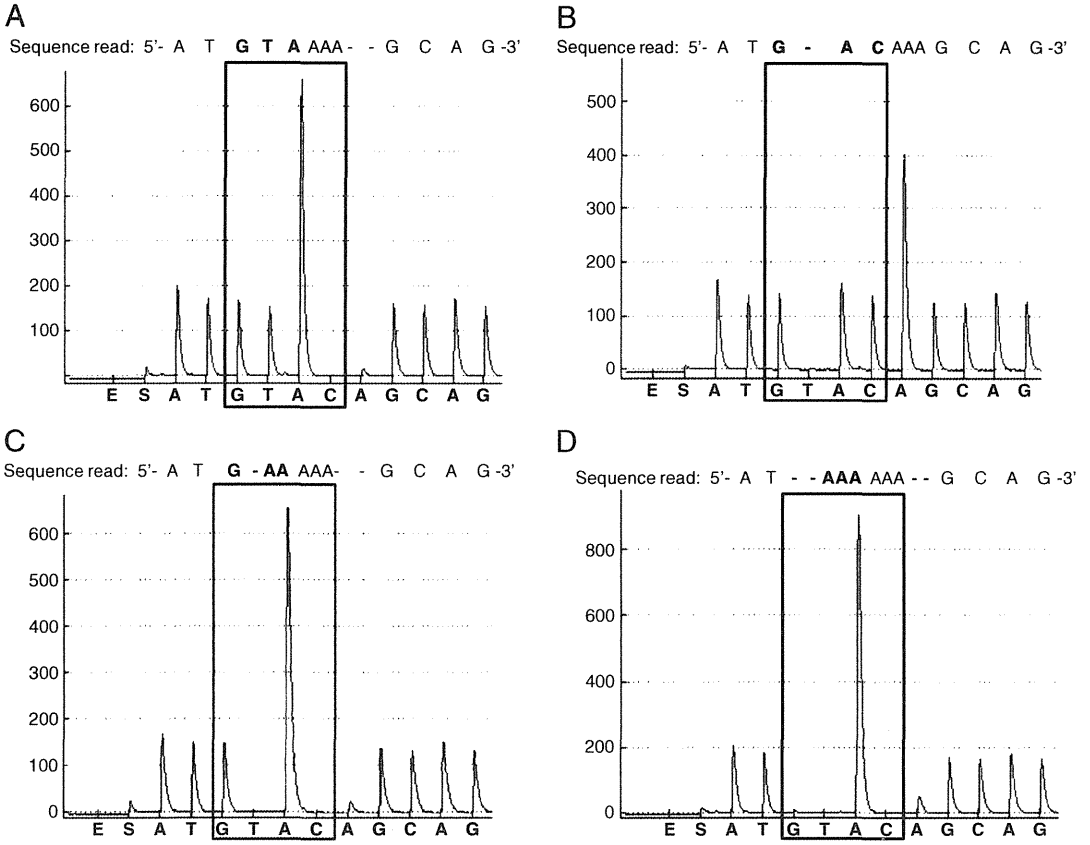

Fig. 2. Four pyrogram patterns of the 12-bp sequence (nucleotide positions: 104–115) in the $bla_{OXA\text{-}51\text{-}like}$ gene. Bold text indicates the unique sequence region (nucleotide positions: 106–108). Characteristic profiles used for discrimination are boxed. (A) International clone II lineage pattern. Sequence of nucleotide positions 106–108: GTA. (B), (C), and (D) Non-international clone II lineage patterns. The sequence of nucleotide positions 106–108 was either GAC, GAA, or AAA, respectively.

2006). These were clinically isolated between 2000 and 2011. PCR-amplification of the gene was negative for all of these 55 isolates. Based on these findings, we set the GTA sequence as the marker of the international clone II lineage of *A. baumannii*, and established a pyrosequencing method for detecting this sequence.

PCR and sequence primers were designed using Pyrosequencing™ Assay Design software ver. 2.0 (SNP/SQA software; QIAGEN, Hilden, Germany). DNA fragments (172 bp) of $bla_{OXA\text{-}51\text{-}like}$ genes were amplified in 15-μL reaction mixtures containing 1.25 U *Ex Taq* (TaKaRa Bio, Shiga, Japan), 0.2 μM forward primer (5′-ATCCAAATCACAGCGCTTCAA-3′), 0.2 μM 5′-biotinated reverse primer (5′-biotin-TTGAAGGTCGAAGCAGG TACATA-3′), 0.2 mM each dNTPs, 2 mM $MgCl_2$, and 1 μL template DNA. The PCR program consisted of an initial denaturation step at 94 °C for 2 min, followed by 30 cycles, each consisting of DNA denaturation at 94 °C for 30 sec, primer annealing at 58 °C for 30 sec, and primer extension at 72 °C for 30 sec, with a final extension step at 72 °C for 5 min. Amplicons were checked by agarose gel-electrophoresis and the biotinylated PCR products then immobilized using Streptavidin Sepharose™ High Performance beads (GE Healthcare, Uppsala, Sweden), and processed to yield ssDNA for pyrosequencing using the PyroMark™ Vacuum Prep Workstation (QIAGEN), according to manufacturer's instructions. Pyrosequencing was performed using PyroMark™ Gold Q24 Reagents (QIAGEN) and the sequence primer 5′-GCGCTTCAAAATCTG-3′ with the PyroMark™ Q24 system (QIAGEN), according to manufacturer's instructions. The dispensation order of dNTPs was set to ATGTACAGCAG. The sequence primer region and the pyrosequencing region are shown in Fig. 1. By the pyrosequencing assay, *A. baumannii* isolates were successfully classified into four groups. Pyrogram of the $bla_{OXA\text{-}51\text{-}like}$ genes of all the international clone II isolates tested consistently demonstrated the GTA sequence pattern at nucleotide positions 106–108 (Fig. 2A, Table 1), whereas pyrograms of the $bla_{OXA\text{-}51\text{-}like}$ genes of the non-international clone II lineages demonstrated either of GAC, GAA, or AAA sequence patterns (Figs. 2B–D, Table 1).

In conclusion, we found that *A. baumannii* international clone II possesses a unique GTA sequence at position 106–108 of the $bla_{OXA\text{-}51\text{-}like}$ genes. After preparation of the PCR products with biotinylated primers, the sequence was detected easily by pyrosequencing, within 15 min. Of course the conventional PCR and nucleotide sequencing analyses would be an alternative way when pyrosequencing equipments are not available. Since this method depends on SNPs in a single gene, it could be susceptible to genetic drift or horizontal gene transfer. Nevertheless, we have not encountered any such exception to date. The conventional MLST would be indeed the gold standard for precise genetic typing, but we believe the pyrosequencing method would become a very practical primary screening tool to discriminate the international clone II lineage.

This work was supported by grants H21-Shinkou-Ippan-008 and H24-Shinkou-Ippan-010 from the Ministry of Health, Labour and Welfare of Japan. We are grateful to all of the participating medical institutions for providing bacterial isolates and clinical information, and to Kumiko Kai, Yoshie Taki, and Yumiko Yoshimura for technical assistance. We also thank the management of the MLST database (http://www.pasteur.fr/mlst and http://pubmlst.org/abaumannii/).

Supplementary data to this article can be found online at http://dx.doi.org/10.1016/j.mimet.2013.05.014.

References

Bartual, S.G., Seifert, H., Hippler, C., Luzon, M.A., Wisplinghoff, H., Rodriguez-Valera, F., 2005. Development of a multilocus sequence typing scheme for characterization of clinical isolates of *Acinetobacter baumannii*. J. Clin. Microbiol. 43, 4382–4390.

Diancourt, L., Passet, V., Nemec, A., Dijkshoorn, L., Brisse, A., 2010. The population structure of *Acinetobacter baumannii*: expanding multiresistant clones from an ancestral susceptible genetic pool. PLoS One 5, e10034.

Dijkshoorn, L., Aucken, H., Gerner-Smidt, P., Janssen, P., Kaufmann, M.E., Garaizar, J., Ursing, J., Pitt, T.L., 1996. Comparison of outbreak and nonoutbreak *Acinetobacter baumannii* strains by genotypic and phenotypic methods. J. Clin. Microbiol. 34, 1519–1525.

Dolzani, L., Tonin, E., Lagatolla, C., Prandin, L., Monti-Bragadin, C., 1995. Identification of *Acinetobacter* isolates in the *A. calcoaceticus-A. baumannii* complex by restriction analysis of the 16S-23S rRNA intergenic spacer sequences. J. Clin. Microbiol. 33, 1108–1113.

Evans, B.A., Hamouda, A., Towner, K.J., Amyes, S.G., 2008. OXA-51-like β-lactamases and their association with particular epidemic lineages of *Acinetobacter baumannii*. Clin. Microbiol. Infect. 14, 268–275.

Hamouda, A., Evans, B.A., Towner, K.J., Amyes, S.G., 2010. Characterization of epidemiology unrelated *Acinetobacter baumannii* isolates from four continents by use of multilocus sequence typing, pulsed-field gel electrophoresis, and sequence-based typing of $bla_{\text{OXA-51-like}}$ genes. J. Clin. Microbiol. 48, 2476–2483.

Héritier, C., Poirel, L., Fournier, P.E., Claverie, J.M., Raoult, D., Nordmann, P., 2005. Characterization of the naturally occurring oxacillinase of *Acinetobacter baumannii*. Antimicrob. Agents Chemother. 49, 4174–4179.

Higgins, P.G., Dammhayn, C., Hackel, M., Seifert, H., 2010. Global spread of carbapenem-resistant *Acinetobacter baumannii*. J. Antimicrob. Chemother. 65, 233–238.

Jones, C.H., Ruzin, A., Tuckman, M., Visalli, M.A., Petersen, P.J., Bradford, P.A., 2009. Pyrosequencing using the single-nucleotide polymorphism protocol for rapid determination of TEM- and SHV-type extended-spectrum β-lactamases in clinical isolates and identification of the novel β-lactamase genes $bla_{\text{SHV-48}}$, $bla_{\text{SHV-105}}$, and $bla_{\text{TEM-155}}$. Antimicrob. Agents Chemother. 53, 977–986.

La Scola, B., Gundi, V.A.K.B., Khamis, A., Raoult, D., 2006. Sequencing of the *rpoB* gene and flanking spacers for molecular identification of *Acinetobacter* species. J. Clin. Microbiol. 44, 827–832.

Peleg, A.Y., Seifert, H., Paterson, D.L., 2008. *Acinetobacter baumannii*: Emergence of a successful pathogen. Clin. Microbiol. Rev. 21, 538–582.

Ronaghi, M., Uhlen, M., Nyren, P., 1998. A sequencing method based on real-time pyrophosphate. Science 281, 363–375.

Spuesens, E.B., Hoogenboezem, T., Sluijter, M., Hartwig, N.G., van Rossum, A.M., Vink, C., 2010. Macrolide resistance determination and molecular typing of *Mycoplasma pneumoniae* by pyrosequencing. J. Microbiol. Methods 82, 214–222.

Turton, J.F., Gabriel, S.N., Valderrey, C., Kaufmann, M.E., Pitt, T.L., 2007. Use of sequence-based typing and multiplex PCR to identify clonal lineages of outbreak strains of *Acinetobacter baumannii*. Clin. Microbiol. Infect. 13, 807–815.

Zander, E., Nemec, A., Seifert, H., Higgins, P.G., 2012. Association between β-lactamase-encoding $bla_{\text{OXA-51-like}}$ variants and DiversiLab rep-PCR-based typing of *Acinetobacter baumannii* isolates. J. Clin. Microbiol. 50, 1900–1904.

Zarrilli, R., Pournaras, S., Giannouli, M., Tsakris, A., 2013. Global evolution of multidrug-resistant *Acinetobacter baumannii* clonal lineages. Int. J. Antimicrob. Agents 41, 11–19.

Journal of Clinical Microbiology

Helicobacter cinaedi and Helicobacter fennelliae Transmission in a Hospital from 2008 to 2012

Emiko Rimbara, Shigetarou Mori, Hyun Kim, Mari Matsui, Satowa Suzuki, Shunji Takahashi, Satoshi Yamamoto, Masaya Mukai and Keigo Shibayama

J. Clin. Microbiol. 2013, 51(7):2439. DOI: 10.1128/JCM.01035-13.
Published Ahead of Print 8 May 2013.

JCM
Journals.ASM.org

Helicobacter cinaedi and *Helicobacter fennelliae* Transmission in a Hospital from 2008 to 2012

Emiko Rimbara,[a] Shigetarou Mori,[a] Hyun Kim,[a] Mari Matsui,[a] Satowa Suzuki,[a] Shunji Takahashi,[b] Satoshi Yamamoto,[b] Masaya Mukai,[b] Keigo Shibayama[a]

Department of Bacteriology II, National Institute of Infectious Diseases, Musashimurayama-shi, Tokyo, Japan[a]; Sapporo City General Hospital, Chuo-ku, Sapporo, Japan[b]

Forty-six *Helicobacter cinaedi* isolates from the same hospital were analyzed by multilocus sequence typing. Most *H. cinaedi* isolates exhibited clonal complex 9 and were mainly isolated from immunocompromised patients in the same ward. Three *Helicobacter fennelliae* isolates were obtained from the same ward and exhibited the same pulsed-field gel electrophoresis patterns. All isolates were resistant to clarithromycin and ciprofloxacin. *H. cinaedi* and *H. fennelliae* must be carefully monitored to prevent nosocomial infection.

Helicobacter cinaedi and *H. fennelliae* are enterohepatic *Helicobacter* species that inhabit the colons of humans and animals. Isolation of *H. cinaedi* and *H. fennelliae* has been reported sporadically (1–10), although reports of *H. cinaedi* are increasing in frequency. The transmission route of *H. cinaedi* is unclear. Since it is prevalent in animals such as dogs and hamsters, these domestic pets may be a natural reservoir for *H. cinaedi* infection in humans (11). However, an association between animals and *H. cinaedi* infection has not been demonstrated. *H. cinaedi* infection is frequent in bacteremia in immunocompromised hosts; therefore, the pathogen may be prevalent in the human colon and invade the blood when the host's immune system is weakened.

In 2008, we reported nosocomial infection with *H. cinaedi* in our hospital (12). We developed a multilocus sequence typing (MLST) method for *H. cinaedi* strains by comparing the results of MLST and pulsed-field gel electrophoresis (PFGE) and confirmed that most *H. cinaedi* isolates from this outbreak were identical (13). After the outbreak, we isolated *Helicobacter* spp. from patients in this hospital to follow the path of *H. cinaedi* infection. In this study, we obtained *H. cinaedi* and *H. fennelliae* isolates from the same hospital for 5 years: the isolates were typed, and their antimicrobial susceptibilities were determined.

Helicobacter isolates were collected at Sapporo City General Hospital in Sapporo, Japan, during 2008 to 2012. *Helicobacter* spp. were isolated from 3 to 8 ml blood in Bactec Plus aerobic/F culture vials (Becton, Dickinson and Company, Franklin Lakes, NJ) after incubation for 3 to 8 days. The isolates were recovered by culture on sheep blood (T) (with Trypticase soy, catalog no. 251148; (Becton, Dickinson and Company, Japan) under microaerobic conditions (AnaeroPack; Mitsubishi Gas Chemical Company, Inc., Tokyo, Japan) for 7 days at 35°C. Isolates from feces were obtained from rectal swabs using Transystem (Copan Diagnostics, Inc., Murrieta, CA) by culture on modified Skirrow's agar plates (Nissui Pharmaceutical Co., Ltd., Tokyo, Japan) under microaerobic conditions (AnaeroPack) for 7 days. The isolates were identified by morphological analysis and DNA sequencing of the 16S rRNA and the 23S rRNA genes. All *Helicobacter* isolates were subcultured in brucella agar (Becton, Dickinson) with 5% horse blood under microaerobic conditions with hydrogen obtained by the gas replacement method using an anaerobic gas mixture (H_2, 10%; CO_2, 10%; and N_2, 80%). During 2008 to 2012, 46 *H. cinaedi* isolates were obtained from different inpatients. Twelve *H. cinaedi* isolates were obtained in 2008; these were described previously (13). Since then, 12, 16, and 5 isolates were obtained in 2009, 2010, and 2011, respectively, and 1 *H. cinaedi* isolate was obtained in 2012; these are described here. Of 46 *H. cinaedi* isolates, 26 were obtained from females and 20 from males. The mean age of the *H. cinaedi*-infected patients was 60.9 years (range, 32 to 79 years). *H. cinaedi*-infected patients had diseases such as malignant lymphoma ($n = 22$), acute lymphoid leukemia ($n = 2$), acute myelogenous leukemia ($n = 3$), autoimmune disease ($n = 5$), myeloma ($n = 2$), adult T-cell leukemia ($n = 1$), nonhematological malignancy ($n = 9$), chronic renal failure ($n = 1$), and ischemic enteritis ($n = 1$). Eight of the *H. cinaedi* isolates were from feces; all others were from blood. Five (10.9%) patients had cellulitis. Of the 46 *H. cinaedi* isolates, 35 were obtained from patients in ward B on the 5th floor and another 6 were from patients in ward C on the same floor. Ward B is mainly reserved for immunocompromised patients; therefore, a weakened immune system is a certain risk factor for *H. cinaedi* infection.

MLST was performed as described previously (13). All se-

TABLE 1 Sequence types and allelic profiles of *H. cinaedi* isolates

Sequence type	Clonal complex	No. (%) of isolates	Allelic profile (allele no.)						
			23S rRNA	*ppa*	*aspA*	*aroE*	*atpA*	*tkt*	*cdtB*
ST2	CC1	1 (2.2)	1	1	1	1	1	4	2
ST3	CC1	4 (8.7)	1	1	1	1	1	4	1
ST4	CC4	1 (2.2)	3	3	3	1	2	2	1
ST10	CC9	26 (56.5)	4	2	2	2	2	1	2
ST11	CC9	9 (19.6)	2	2	2	2	2	1	2
ST15	CC7	2 (4.3)	4	3	5	4	3	4	1
ST16	CC16	1 (2.2)	4	3	2	2	6	4	3
ST17	CC7	2 (4.3)	4	1	5	4	3	4	1

Received 23 April 2013 **Accepted** 2 May 2013
Published ahead of print 8 May 2013
Address correspondence to Emiko Rimbara, rimbara@nih.go.jp.

doi:10.1128/JCM.01035-13

TABLE 2 Relationship between the clonal complex of *H. cinaedi* isolates and the wards from which they were isolated

Floor	Ward	No. (%) of *H. cinaedi* isolates that belonged to:	
		CC9 (n = 35)	Non-CC9 (n = 11)
4th	A	1 (2.9)	0 (0.0)
5th	B	31 (88.6)	4 (36.4)
5th	C	2 (5.7)	4 (36.4)
6th	D	1 (2.9)	1 (9.1)
10th	E	0 (0.0)	1 (9.1)
2nd	Outpatient	0 (0.0)	1 (9.1)

quences were registered in the *H. cinaedi* MLST Database (http://pubmlst.org/hcinaedi/); the allele number, sequence type (ST), and clonal complex (CC) were also defined by the MLST database and the eBURST software program (http://eburst.mlst.net/). As shown in Table 1, MLST analysis divided the 46 *H. cinaedi* isolates into 8 STs and 5 CC categories. Since CC9 (ST10 and ST11) was the most prevalent isolate from this hospital, the isolates were divided into 2 groups: those that belonged to CC9, and those that did not (non-CC9). The wards were compared between groups (Table 2). Of 35 CC9 isolates, 31 (88.6%) were isolated in ward B. Non-CC9 isolates were mainly from wards B and C and were isolated sporadically from other wards. The time courses of isolation of CC9 *H. cinaedi* strains during 2008 to 2012 are shown in Fig. 1. Once CC9 was identified in ward B, it was consistently found in other patients. Among these isolates, ST11 was isolated only in 2008 (n = 8) and 2009 (n = 1). ST10 was isolated every year from 2008 to 2012. Isolates belonging to other CCs were sporadically isolated from different wards during 2008 to 2012. We previously demonstrated that the CC9 strains possessed the same PFGE pattern (13). Therefore, the CC9 isolates have likely been continuously transmitted from patient to patient. To understand why CC9 was prevalent in this hospital, the prevalence of CC9 in each patient's characteristics was compared by Fisher's exact test using GraphPad Prism software (GraphPad Software, Inc., La Jolla, CA); however, no significant differences were observed: 78% (21/27) were found in females versus 74% (14/19) in males (P = 1.000); 79% (30/38) of were from blood versus 63% (5/8) from feces (P = 0.153); 76% (13/17) were found in patients aged >65 years versus 76% (22/29) in patients aged <65 years (P = 1.000); and 80% (4/5) were found in cellulitis-positive patients versus 76% (31/41) in cellulitis-negative patients (P = 0.420). Therefore, *H. cinaedi* CC9 isolates may possess a specific factor for transmission or pathogenicity. *H. cinaedi* expresses cytolethal distending toxin (CDT), but other pathogenetic factors have not been identified. Further investigation of these pathogenetic factors may explain why *H. cinaedi* CC9 is prevalent in this hospital.

H. fennelliae (n = 3) isolates obtained from different patients at the same hospital in July 2011, August 2011, and February 2012 were also analyzed. Two isolates were from the blood of patients with malignant lymphoma (n = 2), and 1 isolate was from the blood of a patient with autoimmune disease (n = 1). Three isolates shared strong sequence identity in the 16S (97%) and 23S (96%) RNA sequences of *H. fennelliae* CCUG18820 and low sequence identity in the 16S and 23S rRNA sequences of *H. cinaedi* CCUG18818. These isolates were also tested by API Campy (bioMérieux) and verified as *H. fennelliae*. To our knowledge, *H. fennelliae* isolation from humans in Japan has not been reported previously. All isolates were obtained from patients in ward B. PFGE for *H. fennelliae* was performed with 3 restriction enzymes (HincII, XhoI, and SmaI) according to the method developed for *H. cinaedi* (13); the restriction patterns were identical between all isolates from the same hospital, while the patterns were different from *H. fennelliae* CCUG18820 (Fig. 2). We also amplified 11 housekeeping genes and confirmed that these sequences were the same in each isolate (data not shown). Therefore, *H. fennelliae* is most likely transferred from patient to patient, as is *H. cinaedi*. All *H. fennelliae* isolates were obtained from ward B; therefore, a weakened immune system could be a risk factor for *H. fennelliae* infection. *H. fennelliae* lacks the CDT that drives virulence in *H. cinaedi* (14). However, the clinical manifestations and backgrounds of *H. fennelliae*-infected and *H. cinaedi*-infected patients were similar. Since the number of *H. fennelliae*-infected patients in this study is small, further investigation is needed to identify the differences in *H. cinaedi* and *H. fennelliae* pathogenicities.

The antimicrobial susceptibilities of *H. cinaedi* and *H. fennelliae* isolates were measured by the agar dilution method (13) and

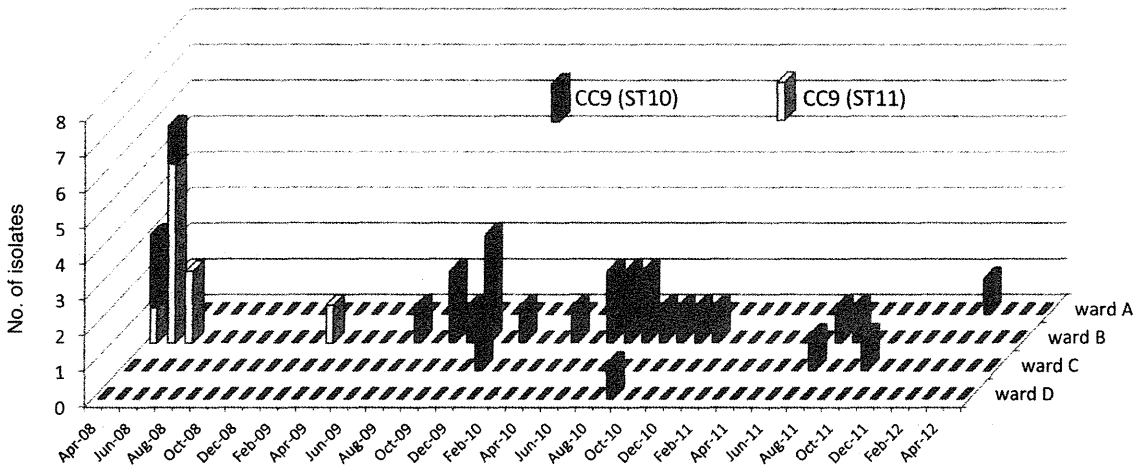

FIG 1 Time course of CC9 *H. cinaedi* isolation.

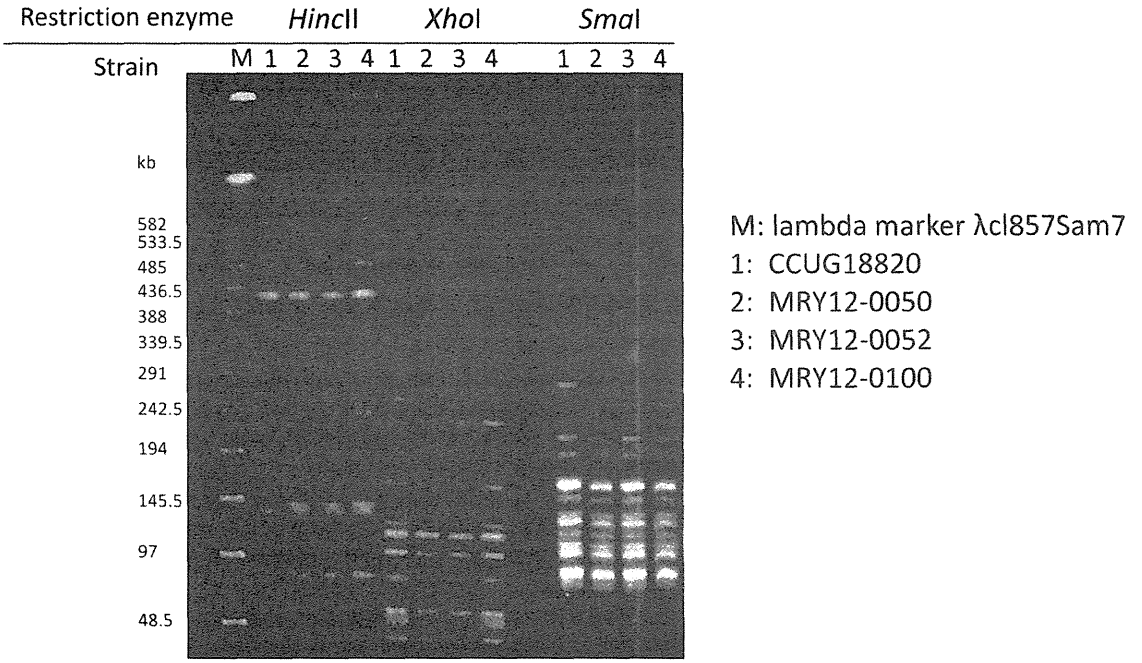

FIG 2 PFGE patterns of 3 *H. fennelliae* isolates from different patients in the same hospital.

are shown in Table 3. All isolates had high MICs for ciprofloxacin and clarithromycin, consistent with prior findings (13). The MIC level of clarithromycin was lower in *H. fennelliae* (8 mg/liter) than that in *H. cinaedi* (MIC_{90}, >128 mg/liter). To determine the mechanism of ciprofloxacin resistance, GyrA and GyrB were sequenced in all *H. cinaedi* and *H. fennelliae* isolates. Compared to *H. cinaedi* CCUG18818, which is susceptible to ciprofloxacin, the *H. cinaedi* isolates possessed mutations in GyrA and GyrB. All mutation patterns and MICs of ciprofloxacin are shown in Table 4. *H. cinaedi* strains with mutations at position 84 in GyrA and position 423 or 442 in GyrB or 2 mutations at positions 84 and 88 in GyrA tended to exhibit high MICs for ciprofloxacin in comparison to isolates with a mutation at GyrA position 84. Since mutations in GyrB confer high-level resistance to fluoroquinolones in *H. pylori* and other species (15), the mutation in GyrB likely confers high-level resistance to ciprofloxacin in *H. cinaedi*. In the *H. fennelliae* isolates, the residue at position 86 of GyrA that corresponded to Thr84 in *H. cinaedi* was lysine. It has been previously shown that ciprofloxacin-susceptible *H. fennelliae* strains possess a threonine at position 84 (16). Therefore, the mutation at position 86 could be the major factor that decreases susceptibility to ciprofloxacin in *H. fennelliae*. The 23S rRNA gene sequences were analyzed in all isolates to identify clarithromycin resistance. All *H. cinaedi* isolates possessed an adenine-to-guanine mutation at position 2018, corresponding to position 2143 of the 23S rRNA gene in *Helicobacter pylori*, which confers clarithromycin resistance in that species. Three *H. fennelliae* isolates had no mutation at position 2327, which corresponds to position 2018 in *H. cinaedi* and position 2143 in *H. pylori*. However, the *H. fennelliae* isolates carried an adenine-to-guanine mutation at position 2879, corresponding to position 2694 of the 23S rRNA gene in *H. pylori*, conferring low-level resistance to clarithromycin (17). This mutation was not observed in *H. fennelliae* CCUG18820, which was susceptible to clarithromycin (0.125 mg/liter). Thus, clarithromycin resistance in the *H. fennelliae* isolates is likely due to mutation at position 2879 of 23S rRNA.

TABLE 3 MICs of *H. cinaedi* and *H. fennelliae* isolates from a hospital in Japan

Isolate and parameter[a]	MIC (mg/liter) of:					
	Amoxicillin	Imipenem	Clarithromycin	Ciprofloxacin	Minocycline	Gentamicin
H. cinaedi						
Clinical isolates (n = 46)						
Range	0.5–32	0.031–0.25	2–>128	16–128	0.016–0.25	0.25–1
50%	4	0.063	64	64	0.063	0.5
90%	8	0.125	>128	128	0.125	0.5
CCUG18818	8	0.063	0.008	0.25	0.25	0.25
H. fennelliae						
Clinical isolates (n = 3), range	1–2	0.031	8	64–>128	0.063–0.125	0.25–0.5
CCUG18820	1	0.031	0.125	0.5	0.125	0.5

[a] 50% and 90%, MIC_{50} and MIC_{90}, respectively.